Spatio-temporal modeling for overactuated motion control

Tacx, Paul; van de Vosse, Matthijs; Voorhoeve, Robbert; Witvoet, Gert; Heertjes, Marcel; Oomen, Tom

Important note
To cite this publication, please use the final published version (if applicable).
Please check the document version above.

Spatio-temporal modeling for overactuated motion control☆

Paul Tacx [a],[*], Matthijs van de Vosse [a], Robbert Voorhoeve [b], Gert Witvoet [a],[b], Marcel Heertjes [a],[c],
Tom Oomen [a],[d]

[a] *Department of Mechanical Engineering, Eindhoven University of Technology, Eindhoven, The Netherlands*
[b] *TNO, Optomechatronics Department, Delft, The Netherlands*
[c] *ASML, Development and Engineering, Mechatronics and Measurement Systems, Veldhoven, The Netherlands*
[d] *Faculty of Mechanical, Maritime, and Materials Engineering, Delft University of Technology, Delft, The Netherlands*

ARTICLE INFO

ABSTRACT

Increasingly stringent performance requirements for motion systems necessitate explicit control of the flexible dynamic behavior. The aim of this paper is to present an approach to identify spatio-temporal models of overactuated mechatronic systems with a limited number of spatially distributed sensors. The proposed approach exploits the modal modeling framework and exploits the symmetry in modal models to enhance the spatial resolution of the identified spatially-sampled modal models. Spatio-temporal models are identified by updating prior finite element method-based models based on the identified extended modal models. The experimental results illustrate the effectiveness of the proposed approach for the identification of complex position-dependent mechanical systems.

1. Introduction

Stringent demands regarding performance in mechatronic systems require the flexible dynamic behavior to be addressed explicitly in the control design [1–3]. Applications include, e.g., adaptive optics in satellite communication and astronomy [4–7] and motion stages in the semiconductor industry [8,9]. Traditionally, the flexible dynamics in these mechatronic applications are not considered explicitly in the frequency range relevant for control [10–13]. This enabled decentralized control through, e.g., decoupling of the rigid-body dynamics in wafer stages and static influence functions in adaptive optics [5,8]. Furthermore, if these rigid-body/static approximations are valid, the spatial system behavior can be derived easily from static extrapolation. However, to meet stringent demands regarding performance and design requirements, a paradigm shift in the design philosophy of next-generation mechatronic systems resulting in, e.g., lightweight and flexible stage design and increasingly large adaptive secondary mirrors [4,6,14]. This leads to the situation where next-generation mechatronic systems exhibit flexible dynamic behavior within the frequency range that is relevant for control which limits the maximum achievable bandwidth and the use of static extrapolations. To actively manage the flexible dynamic behavior through advanced control techniques, these systems will be equipped with many spatially distributed actuators and sensors, i.e., overactuation and oversensing.

The spatio-temporal nature of the flexible dynamics in next-generation overactuated mechatronic systems can be actively managed by exploiting a large number of spatially distributed actuators and sensors. The flexible dynamic behavior in such mechatronic systems leads to inherently spatio-temporal system behavior. At the same time, the measured positions do not necessarily coincide with the positions of interest. Also, the number of sensors that measure the deflection of the deformable mirror is limited with respect to the number of actuators. Approaches that deal with the resulting spatial–temporal control problems are inferential control [15], control of Port-Hamiltonian systems [16,17], and spatial vibration control [3]. These approaches heavily rely on accurate modeling techniques that capture the spatio-temporal nature of the flexible dynamic behavior [14,18].

Traditional parametric and non-parametric identification approaches aim to identify the temporal dynamics, i.e., input–output behavior, of the flexible dynamic behavior [8]. In [19], a modeling method tailored to inferential control is proposed. However, this method requires at least one measurement at the point of interest, which is generally not an easy task.

The introduction of parameter-varying control strategies spurred the development of Linear Parameter-Varying (LPV) system identification techniques [20–22]. These techniques mainly focused on black-box

---

modeling approaches [23,24]. However, the combination of high-order spatial and temporal dynamics in next-generation mechatronic systems leads to high model complexity and significant user intervention when using these black-box LPV modeling approaches.

Alternatively, methods have been developed that employ prior system knowledge to model the spatio-temporal system behavior. The flexible dynamics can be described by partial differential equations that can be identified using techniques presented in, e.g., [25–27]. However, these techniques are not directly suited to next-generation overactuated mechatronic systems due to the high level of user intervention and high system complexity due to, i.e., advanced three-dimensional geometries, large number of actuators, and high sampling rate.

In [28], an approach is proposed to identify spatio-temporal mechanical models of wafer stages. Essentially, a modal model is identified based on frequency response data. The spatio-temporal model is constructed by interpolating the identified mode shape vectors through a thin-plate spline. However, the method is only based on the sensor data and the thin-plate spline may not have the fidelity to capture the spatial system behavior which limits the accuracy of the interpolation. In addition, the identification step does not employ additional prior system knowledge about the mode shape vectors and eigenfrequencies. Similarly, in [29,30], a first-principles modeling approach is pursued for feedforward design in deformable mirror systems. However, first-principles-based approaches often not have the fidelity to describe the complex nature of the flexible dynamics.

Prior finite element method (FEM) models of mechatronic systems are widely used to model spatio-temporal system dynamics [31–34]. Although these FEM models have a high spatial resolution, in practice, these models mismatch with the true system dynamics in terms of, e.g., overestimation of the stiffness resulting in overestimated eigenfrequencies, and these models do not capture variations across systems due to manufacturing tolerances. This is mainly attributed to simplifications of the true geometry in the FEM model, and additional non-modeled artifacts in the hardware and uncertainty in the physical properties. As a consequence, these models may not be sufficiently accurate for control of overactuated mechatronic systems.

Alternatively, in the field of structural analysis, model updating is employed to correct the FEM models based on the responses of the true structure. Various model updating techniques are presented in the literature including techniques to update physical parameters, see, e.g., [35,36] for an overview. For instance, in [37–39], approaches are presented to update model parameters based on modal models. However, the use of these methods is not well established in the field of identification and control of mechatronic systems. As a result, these approaches are generally not unified, i.e., these approaches do not describe the identification of the modal model, and are based on the finite number of sensors, which limits the quality of the updated model. Also, in [40–42], methods are presented to update modal parameters directly from time and frequency domain data. However, these methods lead to significant user intervention and are computationally expensive for mechatronic systems that have high sampling rates. Despite the established use of model updating algorithms in structural analysis, their use for control of mechatronic systems remains limited.

Although important developments have progressed spatio-temporal system identification for control, at present, existing approaches seem less tailored to control of overactuated mechatronic systems. The aim of this paper is to present a systematic method for constructing spatio-temporal models for overactuated control by combining concepts from the field of identification and control of mechatronic systems and the field of structural analysis. The proposed method is unified in the sense that all the steps from frequency response function measurements to the identification of spatio-temporal models are included. The key step in this paper is to employ prior system knowledge. An important observation is the fact that the system dynamics are dominated by structural dynamics that are typically induced by a single moving body

with small deflections. The first step in the construction of the spatio-temporal model is to identify a spatially sampled modal model that captures the input–output behavior. A dedicated algorithm is proposed to identify modal models from frequency response function estimates. The second step is concerned with enhancing the spatial resolution of the obtained modal model by exploiting the symmetric nature of the mode shape vectors at actuator and sensor level [43]. Related work includes the field of experimental modal analysis and the Maxwell–Betti reciprocal theorem, see e.g. [44–47]. The third step is concerned with the construction of the spatio-temporal model. The approach is based on combining the prior FEM model with the experimentally determined extended modal model through model updating techniques from the field of structural analysis. The main contributions of the paper are the following.

C1 Unified approach to identify the spatio-temporal dynamics of overactuated mechatronic systems with a limited number of sensors.

  C1.1 A systematic approach for identifying modal models of overactuated mechatronic systems.
  C1.2 Construction of the spatially enhanced extended modal models at the unmeasured actuator locations.
  C1.3 Spatio-temporal modeling approach by updating the prior FEM model using the experimentally determined extended modal model.

C2 An experimental case study with an experimental overactuated beam setup which is considered representative for several aspects of overactuated mechatronic systems confirms the effectiveness of the proposed approaches.

This paper is organized as follows. In Section 2, the main problem and the experimental setup are introduced. In Section 3, the modal modeling framework and the approach are outlined. In Section 5, the modal identification approach and the formulation of the extended modal model are introduced. In Section 6, the spatio-temporal model is constructed using the extended modal model. In Section 8, a discussion of the proposed results is provided In Section 9, the conclusions are formulated and an outlook for future research is presented.

2. Problem formulation

In this section, the class of overactuated mechatronic systems and the related control challenges considered in this paper are introduced. Also, the spatio-temporal modeling problem considered in this paper is formulated.

2.1. Inferential control challenge

Next-generation mechatronic systems are envisaged to exhibit flexible dynamic behavior within the frequency range that is relevant for control. The flexible dynamic behavior leads to inherent spatio-temporal system dynamics, which needs to be controlled with a large number of spatially distributed actuators. Two main consequences are associated with the spatio-temporal system dynamics. First, to validate the next-generation designs, models are required to analyze and provide insight into the underlying system dynamics. Second, the measured variables do not necessarily coincide with the performance variables resulting in an inferential control problem, see, e.g., [15,19] for control methods for such problems. As a consequence, models are required that capture the spatio-temporal nature of the flexible dynamics to deal with these consequences.
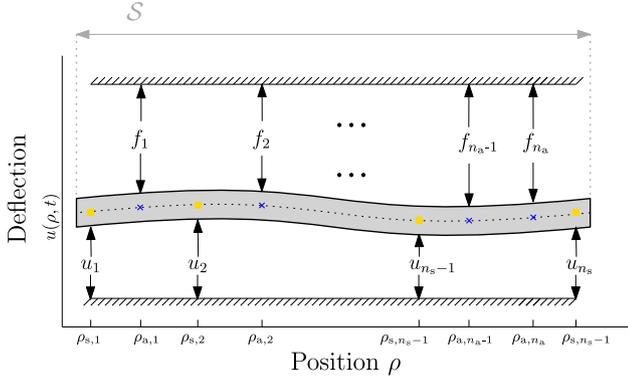
Fig. 1. Two-dimensional schematic representation of an overactuated system. The representation includes n_a actuators (×) that are denoted as F_i, $i \in \{1, \ldots, n_a\}$ and n_s sensors that measure the deflection (▪). The geometry of the system is denoted by the spatial domain S.

2.2. Problem formulation

A schematic overview of an example overactuated system is depicted in Fig. 1. The spatial domain $S \in \mathbb{R}^2$ of the position variable ρ is the two-dimensional in-plane position in the geometry of the flexible body. The main variable of interest is the out-of-plane deflection $u(\rho, t)$ of the flexible body. Measurement data is obtained at a finite number of spatially distributed sensor locations with a large number of spatially distributed actuators

$$G_s : f(t) \mapsto \bar{u}(t) \tag{1}$$

where G_s denotes the overactuated system, $f(t) \in \mathbb{R}^{n_a}$ denotes the actuator forces, and $\bar{u}(t) \in \mathbb{R}^{n_s}$ the deflection measured at the sensors. The number of actuators is denoted by n_a and the in-plane positions of the actuators are denoted by

$$\bar{\rho}_a = \left\{ \rho_{a,1}, \ldots, \rho_{a,n_a} \right\}, \quad \rho_{a,i} \in S, \quad i = 1, \ldots, n_a. \tag{2}$$

The sensor data is obtained with sensors that measure the displacement of the flexible body at n_s distinct locations

$$\bar{u}(t) = \begin{bmatrix} u(\rho_{s,1}, t) & \ldots & u(\rho_{s,n_s}, t) \end{bmatrix}^\top \tag{3}$$

and the in-plane positions of these sensors are stacked into a vector

$$\bar{\rho}_s = \left\{ \rho_{s,1}, \ldots, \rho_{s,n_s} \right\}, \quad \rho_{s,i} \in S, \quad i = 1, \ldots, n_s. \tag{4}$$

Consequently, the deflection of the flexible body can be assessed at a limited number of sensor locations.

The main problem addressed in this paper is to identify a position-dependent model of the form

$$\hat{G}(\rho, t) = \begin{cases} \dot{x}(t) & = Ax(t) + Bf(t), \\ u(\rho, t) & = C(\rho)x(t) \end{cases} \tag{5}$$

where the model $\hat{G}(\rho, t)$ describes the spatio-temporal dynamics of the flexible body. Since the overactuated system G_s is a spatially sampled version, it can be retrieved as a special case. The deflection is assumed to be sufficiently small such that it does not influence the internal dynamics. For this reason, the A matrix is invariant to the position variable ρ. The actuator locations are fixed with respect to the moving body and therefore the B matrix is constant. The system is thus only position-dependent through the C matrix.

While temporal system identification can still be performed with high fidelity due to high sampling rates, the scarcity of spatial data, limited by the number of sensors, restricts the ability to accurately model or interpolate the spatial system dynamics, which leads to degraded inferential control performance. The aim of this paper is to develop a spatio-temporal identification approach that exploits prior mechanical system knowledge to reconstruct the spatio-temporal behavior of overactuated mechatronic systems.

3. Spatio-temporal modeling approach

In this section, the approach for identifying spatio-temporal models of overactuated systems is introduced. First, the modal modeling framework is introduced and used to analyze overactuated mechatronic systems. Second, the approach is presented to identify spatio-temporal models.

3.1. Modeling flexible structures

The key variable is the out-of-plane deflection $u(\rho, t) \in \mathbb{R}$, see Fig. 1, which is defined by partial differential equations of which the solution can be described through space–time-separated basis functions [47],

$$u(\rho, t) = \sum_{k=1}^{n_q} w_k(\rho) q_k(t). \tag{6}$$

The temporal contribution is determined by the generalized coordinates $q_k(t)$ and the spatial contribution is determined by $w_k(\rho)$. The solution in (6) converges to the true deflection for $n_q \to \infty$ for appropriate basis functions. Analytical solutions are not available in general and only exist for specific cases. For this reason, the solution often is limited to FEM models that use a finite set of points in space. Throughout this paper, the nodal coordinates are structured as $q(t) = \begin{bmatrix} q_a(t)^\top q_e(t)^\top \end{bmatrix}^\top$, where $q_a(t)$ contains the nodal coordinates that correspond to the actuator positions $\bar{\rho}_a$ and $q_e(t)$ contain the remaining coordinates, including a fine grid of the spatial coordinate in (37). Given the separation of time and space in (6), the dynamics can be formulated as a coupled set of second-order ordinary differential equations

$$M\ddot{q} + D\dot{q} + Kq = Qf(t) \tag{7}$$

where the mass matrix $M \in \mathbb{R}^{n_q \times n_q}$ is positive definite, $D \in \mathbb{R}^{n_q \times n_q}$ denotes the damping matrix, $K \in \mathbb{R}^{n_q \times n_q}$ the positive semi-definite stiffness matrix, $Q \in \mathbb{R}^{n_q \times n_a}$ the input matrix, and $f(t) \in \mathbb{R}^{n_a \times 1}$ the input function at actuation locations in (2). Because the actuators operate in an absolute setting and the nodal coordinates are structured in a specific form, the input matrix is partitioned as $Q = [I, O]^\top$, where I denotes an identity matrix and O denotes a zero matrix, both of appropriate dimensions.

The problem of finding the values of ω^2 and a non-trivial $\bar{\phi}$ is known as the generalized eigenvalue problem

$$\begin{bmatrix} K - \omega^2 M \end{bmatrix} \bar{\phi} = 0. \tag{8}$$

A nontrivial solution exists if and only if the characteristic polynomial associated with the matrices K and M is equal to zero, i.e., $\det(K - \omega^2 M) = 0$. The characteristic polynomial consists of n_q roots which are denotes throughout as ω_k, $k = 1, \ldots, n_q$. Associated with the eigenfrequencies are the corresponding eigenvectors $\bar{\phi}_k$, $k = 1, \ldots, n_q$, which denote the mode shape vector sampled at the positions of the nodes. Throughout this paper, mass-normalized generalized eigenvectors are considered, i.e.,

$$\bar{\phi}_k M \bar{\phi}_k^\top = I. \tag{9}$$

The scalar function $\phi_k(\rho) : S \mapsto \mathbb{R}$ is the kth mass-normalized mode shape function, which depends on the spatial variable ρ. To improve conciseness of the results, these functions are vectorized as $\bar{\phi}_k$ by evaluating the scalar functions at the spatial locations of the nodal coordinates. Due to the specific ordering of the nodal coordinates, the mode shape vector is partitioned accordingly as $\bar{\phi}_k = \begin{bmatrix} \bar{\phi}_{a,k}^\top & \bar{\phi}_{e,k}^\top \end{bmatrix}^\top$.

The coupled set of differential equations in (7) can be decoupled by introducing the coordinate transformation to modal coordinates, i.e. $q = \Phi\eta$, where $\Phi = \begin{bmatrix} \bar{\phi}_1, \ldots, \bar{\phi}_{n_q} \end{bmatrix}$. Substituting the coordinate transformation and left multiplying (7) with $\Phi^\top$ leads to

$$G_m(\rho) = \begin{cases} I\ddot{\eta} + D_m\dot{\eta} + K_m\eta = \begin{bmatrix} \bar{\phi}_{a,1} \ldots \bar{\phi}_{a,n_q} \end{bmatrix}^\top f(t), & \text{(a)} \\ u(\rho, t) = \sum_{k=1}^{n_m} \phi_k(\rho)\eta_k(t) & \text{(b)} \end{cases} \tag{10}$$

where $D_m = \Phi_a^\top D \Phi_a = \mathrm{diag}\left(d_{m,1}, \ldots, d_{m,n_q}\right)$, $K_m = \Phi_a^\top K \Phi_a = \mathrm{diag}\left(\omega_1^2, \ldots, \omega_{n_q}^2\right)$. In this paper, modal damping is considered which leads to the decoupled set of differential equations in (10)(a) and which is a useful approximation of many lightly-damped systems in practice.

3.2. Spatio-temporal identification approach

Measurement data is obtained at a finite number, n_s, of spatially distributed sensors which are defined by the set $\bar{\rho}_s$. The system dynamics are identified from the obtained experimental data where the model is parameterized in the modal form, i.e., (10)(a), with a limited number of n_m modes. Instead of a continuous position-dependent mode shape function in (10)(b), a spatially sampled system is measured

$$\bar{u}_s(t) = \sum_{k=1}^{n_m} \begin{bmatrix} \phi_k(\rho_{s,1}) \\ \vdots \\ \phi_k(\rho_{s,n_s}) \end{bmatrix} \eta_k(t). \tag{11}$$

The key idea in this paper is to exploit system knowledge to identify spatio-temporal models using a limited number of available sensors that measure the deflection. In particular, since the dynamics are dominated by structural dynamics, the modal modeling framework is exploited and prior FEM models are used. To this end, the first step in the proposed spatio-temporal modeling procedure is to identify the frequency response function in Section 4. A frequency domain approach is pursued since this approach is interpretable from a control perspective and data efficient.

The second step involves the identification of modal models of the form (10)(a) and (11) with a dedicated algorithm in Section 5. Due to the high sampling rates, these models provide an accurate description of the temporal systems dynamics. In contrast, due to the limited number of sensors n_s, these models determine the spatially sampled system behavior with a limited spatial resolution.

In the third step, in Section 5.2, extended modal models are constructed by combining the mode shape vectors sampled at the actuator and sensor locations to enhance the spatial resolution of the modal models. This procedure enables to enhance the spatial resolution without using additional sensors, however, the resolution is still limited by the number of sensors and actuators.

The fourth step is presented in Section 6 where the experimentally determined extended modal models are used to construct spatio-temporal models through prior FEM models. Typically, the latter contain a large number of elements thereby exceeding the number of sensors significantly $n_n \gg n_s$. As a consequence, the deflection function in (10)(b) can be estimated with a large spatial resolution. In this step, prior FEM models are parameterized and updated based on the extended modal models to reconstruct spatio-temporal behavior of overactuated systems. Since this step relies on prior system knowledge, the spatial nature of the dynamics can be determined accurately without the use of a large number of sensors. The proposed approach is graphically shown in Fig. 2. In the following sections, the spatio-temporal modeling approach is presented which constitutes the main contribution of this paper, i.e., Contribution C1.

4. Frequency response function estimation

4.1. Frequency response function estimation

Frequency response function estimation is the first step in identifying the spatio-temporal models. In an experimental setting, experiments are usually conducted with discrete-time signals due to the digital interface. To estimate the frequency response functions, the discrete time excitation signal f, and output $\bar{u}$ in Fig. 3 are measured. These signals are transformed through the Discrete Fourier Transform (DFT) into the frequency domain, which leads to $F^{\langle l\rangle}(v)$ and $\bar{U}^{\langle l\rangle}(v)$, where v
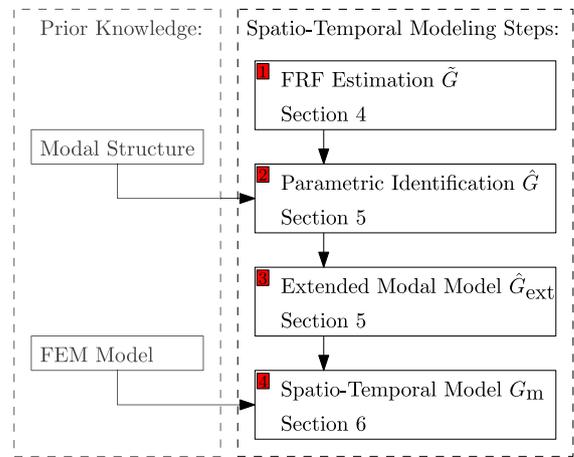
Fig. 2. Schematic overview of the proposed spatio-temporal modeling approach.
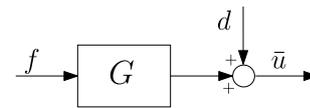
Fig. 3. Open-loop setting of a linear time invariant system with input f, measurement noise d, and output $\bar{u}$.

denotes the vth DFT bin. By performing $l = \{1, \ldots, n_a\}$ experiments, the frequency response function is estimated as

$$\tilde{G}_s(\Omega_v) = \left[\bar{U}^{\langle 1\rangle}(v) \ldots \bar{U}^{\langle n_a\rangle}(v)\right] \left[F^{\langle 1\rangle}(v) \ldots F^{\langle n_a\rangle}(v)\right]^{-1} \tag{12}$$

where the frequency variable at the vth DFT bin is denoted by Ω_v.

Several crucial aspects impact the design and processing of the experiment. Firstly, the noise d represented in Fig. 3 is assumed to be filtered white noise, this ensures that the measured inputs and outputs are normally distributed and have zero mean. Consequently, noise-related estimation errors can be solely characterized by their variance. Secondly, averaging and windowing can be invoked to reduce transient leakage error and noise-related estimation variance. In addition, periodic input signals can further reduce the noise-related estimation variance. Thirdly, a critical condition for the identification approach in (12) is the full rank condition of the excitation matrix $\left[F^{\langle 1\rangle}(v) \ldots F^{\langle n_a\rangle}(v)\right]$, meaning the applied input signals must span the entire input space. This is typically achieved by using n_a independently generated white noise signals or random-phase multisine signals. Fourthly, to facilitate exposition, this paper assumes an open-loop setting for frequency response function estimation. It is important to note that this approach extends to the closed-loop setting as well, see, e.g., [48,49]. Finally, the remainder of the paper adopts a pseudo continuous-time setting (i.e., $\Omega_v = j\omega_v$), see [50, Chapter 8] for details. Any delays introduced in an experimental setting by the zero hold circuitry can be efficiently identified and compensated using existing automated methods or manual data inspection and compensation [51, Section 8.5] [50, Chapter 8]. This allows to perform the subsequent parametric identification procedures in the Laplace domain.

5. Modal model identification

In this section, an approach is presented to identify parametric modal models which describe the input–output behavior. This is an essential step for identifying spatio-temporal models as outlined in Section 3. First, the modal model identification approach is presented, including the parametrization, algorithm, and initial estimate. Second, the spatial resolution of the identified modal models is enhanced by exploiting the symmetry in the modal structure.

5.1. Modal model identification approach

This subsection presents the approach for identifying modal models of the spatially sampled system G_s which constitutes Contribution C1.1. First, the parametrization is outlined, defining the model structure and the identification parameters. Second, the algorithm is introduced which outlines the steps to estimate the parameters from the frequency response function estimate introduced in Section 4.1. Third, the initial condition for the identification algorithm is proposed.

5.1.1. Parametrization

The modeling of the spatio-temporal system dynamics requires the identification of the spatially sampled system G_s in (38). In this paper, a frequency domain-based approach is pursued to identify the parametric model. For this reason, it is essential to formulate a modal parametrization in the frequency domain. A frequency domain-based description of the spatially sampled system given by (10)(a and (11) is defined through the application of the modal expansion theorem

$$\hat{G}_s(s, \theta) = \sum_{k=1}^{n_m} \frac{R_k}{s^2 + d_{m,k}s + \omega_k^2}. \tag{13}$$

Essentially, the modal model in (13) can be interpreted as a summation of modal contributions. Here, R_k denotes the rank-one modal participation matrix that is based on the sampled mode shape vectors and that is defined as

$$R_k = v_k w_k^\top \tag{14}$$

where

$$v_k = \begin{bmatrix} \phi_k(\rho_{s,1}) \\ \vdots \\ \phi_k(\rho_{s,n_s}) \end{bmatrix}, \qquad w_k = \begin{bmatrix} \phi_k(\rho_{a,1}) \\ \vdots \\ \phi_k(\rho_{a,n_a}) \end{bmatrix}. \tag{15}$$

An important observation is that the mode shape vector is encountered twice through v_k and w_k which represent the mode shape vector sampled at the sensor and actuator locations respectively. The parametric modal model in (13) is fully defined by the parameter vector

$$\theta = \text{vec}\left\{\bar{d}_m, \bar{\omega}_m, \Phi_v, \Phi_w\right\} \tag{16}$$

Where the parameter vectors are defined as $\bar{\omega}_m = \left[\omega_{m,1}, \ldots, \omega_{m,n_m}\right]$, $\bar{d}_m = \left[d_{m,1}, \ldots, d_{m,n_m}\right]$. The parameter matrices denote the mode shape vectors sampled at the sensor locations $\Phi_v = \left[v_1, \ldots, v_{n_s}\right]$ and at the actuator locations $\Phi_w = \left[w_1, \ldots, w_{n_a}\right]$. In view of identification for control, low-order models are desired that are sufficiently accurate in the frequency range of interest. This means that only a limited number of modal coordinates n_m is required. Usually, a limited number of modes dominates the system dynamics in the frequency range which is relevant for control. In the case of dominant unmodeled high-order modes, a compliance effect may occur at lower frequencies [52]. While not explicitly included in the current paper, the proposed approach can be readily extended to encompass the residual flexibilities from the unmodeled modes by incorporating a direct feed-through term [53]. The considered modal parametrization in (13) can be trivially transformed to the state-space form in (5) as shown in, e.g., [28].

5.1.2. Algorithm

The key identification aim is to find the parameter vector θ that minimizes the Frobenius norm-based cost function

$$\hat{\theta} = \arg\min_\theta \sum_{v=1}^{N} \left\|\epsilon(\theta, \Omega_v)\right\|_F^2. \tag{17}$$

$$\epsilon(\theta, \Omega_v) = W_s(\Omega_v) \circ \left(W_u(\Omega_v)\left(\tilde{G}_s(\Omega_v) - \hat{G}_s(\theta, \Omega_v)\right)W_f(\Omega_v)\right) \tag{18}$$

Here, $W_s(\Omega_v)$, $W_f(\Omega_v)$, and $W_u(\Omega_v)$ denote the Schur, input, and output filter, respectively, that are frequency-dependent weighting matrices

selected by the control engineer. The symbol $\circ$ denotes the Hadamard product. The optimization in (17) is a nonlinear least-squares problem that is solved iteratively. In this paper, Gauss–Newton iterations are used to solve the optimization problem.

Algorithm 1. Gauss–Newton Iterations Procedure. Given an initial estimate $\theta^{\langle 0 \rangle}$. Compute a new parameter vector by solving the linear least-squares problem for $i = 0, 1, 2, \ldots$

$$\theta^{\langle i+1 \rangle} = \theta^{\langle i \rangle} + \arg\min_{\Delta_\theta} \sum_{v=1}^{N} \left\| \left. \frac{\partial \epsilon(\theta, \omega_v)}{\partial \theta^\top} \right|_{\theta^{\langle i \rangle}} \Delta_\theta + \epsilon(\theta^{\langle i \rangle}, \omega_v) \right\|_F^2 \tag{19}$$

The Gauss–Newton algorithm is known for its efficient and often monotonic convergence to a minimum of the cost function. The obtained minimum is not necessarily the global minimum and depends on the quality of the initial estimate. Traditionally, the Sanathanan-Koerner algorithm (e.g., [28,54]) is used to provide an initial guess for these gradient-based methods, but this adds computational complexity and necessitates additional user intervention.

Remark 1. The weighted least-squares cost function in (17) encompasses control-relevant identification criteria [55, Section A.2]. This allows to explicitly incorporate the control goal into the identification step.

Remark 2. The rank-one property of the modal participation matrix is enforced from the singular value decomposition, i.e., $\tilde{R}_k = U_k \Sigma_k V_k^\top$, such that

$$R_k = \left[U_k\right]^1 \left[\Sigma_k\right]_1^1 \left[V_k\right]_1^\top. \tag{20}$$

The first column and row are denoted by $\left[U_k\right]^1$ and $\left[V_k\right]_1$, respectively. Enforcing the rank-one property in (22) generally works well in practice as will be shown in Section 7.3.

5.1.3. Initial condition

The initial estimate is determined in three steps. First, the initial estimate of resonance frequencies $\bar{\omega}_{m,k}^{\langle 0 \rangle}$ are manually selected from the element-wise Bode magnitude plot. Second, the damping parameters $\bar{d}_{m,k}^{\langle 0 \rangle}$ are estimated by estimating locally a second-order model to several elements of the frequency response estimate that is optimal in the least-squares sense. This approach is also known as the Single DOF (SDOF) approach, see, e.g., [47,56,57]. The values are averaged to obtain an accurate estimate of the global system parameters.

Finally, the initial estimate of the modal participation matrix $R_k^{\langle 0 \rangle}$ in (14) is obtained through the circle fitting method [47]. Essentially, this approach is based on the observation that at the resonance frequency, the response of the mechanical system in (13) is approximately

$$\tilde{G}_s(j\omega_k) \approx \frac{-jR_k}{d_{m,k}\omega_k}. \tag{21}$$

Based on this observation, the frequency response function estimate, and the initial estimate of the resonance and damping parameters, the modal participation matrix is estimated, i.e.,

$$R_k^{\langle 0 \rangle} = d_{m,k}^{\langle 0 \rangle} \omega_{m,k}^{\langle 0 \rangle} \text{Im}\left\{\tilde{G}_s(j\omega_{m,k}^{\langle 0 \rangle})\right\}. \tag{22}$$

The method described by (22) generally works well in practice with a sufficiently high resolution of the frequency response estimate [58]. The rank one property of the modal participation matrix in (22) is enforced by the procedure outlined in Remark 2.

5.2. Extending modal models

The modeling of the spatial component in (10)(b) typically requires a high model complexity. At the same time, only a limited number of n_s sensor locations cover the spatial domain S which limits the quality of the spatial component. In this subsection, an approach is proposed that

allows for the evaluation of the mode shape vector at an increased set of spatial locations by combining sensor and actuator data. This section constitutes Contribution C1.2.

An important observation for the analysis of the modal model is that the modal participation matrix is based on the mode shape vectors in (14). The key idea in this paper is that in the modal description, e.g. (13), the mode shape vectors are encountered twice. Specifically, the mode shape vector is sampled at the sensor and actuator locations. The following theorem is an important step in the reconstruction of these mass-normalized mode shape vectors.

Theorem 1. *If $R_k \in \mathbb{R}^{n_s \times n_a}$ is a rank-one matrix, then R_k can be decomposed into*

$$R_k = \tilde{v}_k \tilde{w}_k^\top, \tag{23}$$

with $\tilde{v}_k \in \mathbb{R}^{n_s}$ and $\tilde{w}_k \in \mathbb{R}^{n_a}$.

Proof. The proof follows from the definition of the matrix rank, see e.g., [59, Section 3.115] and [60, Section 3.6]. $\square$

Thus, every modal participation matrix, e.g., (14), is decomposed into a product of mode shape vectors. The key issue is that the decomposition is not unique. For instance $\alpha \tilde{v}_k^\top \frac{1}{\alpha} \tilde{w}_k^\top$ with any nonzero $\alpha \in \mathbb{R}$ is a solution. Thus, the mode shape vector is unique up to a scaling constant [61]. The following result provides a sufficient design requirement for finding a unique decomposition of the modal participation matrix into mass-normalized mode shape vectors.

Theorem 2. *Let R_k be a rank-one modal participation matrix of a system according to (13) with n_a actuators, n_s sensors. If there exists at least one collocated sensor-actuator pair, i.e., $\rho_{s,i} = \rho_{a,j}$ with $i, j \in \mathbb{N}$, then the decomposition in (15) can be uniquely determined.*

Essentially, Theorem 2 enables the extraction of mass-normalized mode shape vectors by a design requirement, i.e., at least one collocated sensor-actuator pair should be present. A proof of Theorem 2 is provided in Appendix. An additional requirement is that the collocated sensor-actuator pair should not be located at a node of any relevant mode shape.

The key idea in this paper is that in the modal description, e.g. (23), the mode shape vector is encountered twice. Specifically, the mode shape is sampled at the sensor and actuator locations. To enhance the spatial resolution of the modal model, the mode shape vectors sampled at sensor and actuator locations are combined. Consider

$$\hat{\phi}_{\text{ext},k} = \begin{bmatrix} \phi_k(\bar{\rho}_{\text{ext},1}) \\ \vdots \\ \phi_k(\bar{\rho}_{\text{ext},n_{\text{ext}}}) \end{bmatrix} \tag{24}$$

where $\hat{\phi}_{\text{ext},k} \in \mathbb{R}^{n_{\text{ext}}}$ denotes the extended mode shape vector and $\bar{\rho}_{\text{ext}} = \bar{\rho}_a \cup \bar{\rho}_s$ denotes the combined actuator and sensor locations set. The spatial resolution of the extended mode shape vector depends on the number of sensors, actuators, and collocated sensor-actuator pairs, i.e.,

$$n_{\text{ext}} = \text{card}\left(\bar{\rho}_{\text{ext}}\right) \tag{25}$$

where card() denotes the cardinality of a set. Since at least one collocated sensor actuator pair is required in Theorem 2, the ultimately achievable resolution of the combined mode shape vector is bounded by

$$n_s \leq n_{\text{ext}} \leq n_s + n_a - 1. \tag{26}$$

The extended mode shape vector $\hat{\phi}_{\text{ext},k}$ in (24) provides additional information about the spatial nature of the flexible dynamic behavior which is essential for identifying spatio-temporal models.

The interchanging role of sensors and actuators underlying (24) is known as the Betti–Maxwell theorem, see, e.g., [43–45,62]. This interchanging role is exploited in this paper to spatially enhance modal models for spatio-temporal modeling for control.

The combined sampled mode shape vector in (24) allows for the construction of the extended modal model

$$\hat{G}_{\text{ext}}(s) = \sum_{k=1}^{n_m} \frac{\hat{R}_{\text{ext},k}}{s^2 + d_{m,k} s + \omega_k^2}, \tag{27}$$

$$\hat{R}_{\text{ext},k} = \hat{\phi}_{\text{ext},k} \hat{\phi}_{a,k}^\top, \tag{28}$$

which enhances the spatial resolution compared to the modal model in (13).

6. Spatio-temporal modeling

This section presents the approach to identify spatio-temporal models of overactuated motion systems with a limited number of sensors. The spatio-temporal model is constructed by combining the extended modal model with a prior FEM model. The modeling approach is discussed including the parametrization and algorithm.

6.1. Spatio-temporal modeling

In this subsection, a method is presented to construct spatio-temporal models by updating FEM models using the identified extended modal models. This section constitutes Contribution C1.3.

6.1.1. Parametrization

The prior FEM model forms the basis for identifying the spatio-temporal system. An essential step is to parameterize the FEM model based on physical parameters

$$K^{\text{FEM}}(\bar{\alpha}) = K_0^{\text{FEM}} + \sum_{i=1}^{n_\alpha} K_i^{\text{FEM}} \alpha_i \tag{29}$$

$$M^{\text{FEM}}(\bar{\alpha}) = M_0^{\text{FEM}} + \sum_{i=1}^{n_\alpha} M_i^{\text{FEM}} \alpha_i \tag{30}$$

where $\bar{\alpha}$ denotes the parameter vector

$$\bar{\alpha} = \begin{bmatrix} \alpha_1, \ldots, \alpha_{n_\alpha} \end{bmatrix}. \tag{31}$$

that contains the physical update parameters such as, e.g., the elasticity modulus and mass density of certain elements. Notice that the stiffness and mass matrices are assumed to be linear in the parameter vector $\bar{\alpha}$. In this paper, the parameters are updated based on the eigenvalues and mode shape vectors. As a consequence of the parameter-dependent mass and stiffness matrix in (29) and (30), the corresponding eigenfrequencies and mode shape vector depend implicitly on these parameters

$$\tilde{\omega}_k^{\text{FEM}}(\bar{\alpha}) \tilde{\phi}_k^{\text{FEM}}(\bar{\alpha}) \quad k = 1, \ldots, n_q \tag{32}$$

where $\tilde{\omega}_k^{\text{FEM}}(\bar{\alpha})$ denotes the kth eigenfrequency of the FEM model and $\tilde{\phi}_k^{\text{FEM}}(\bar{\alpha})$ denotes the kth mode shape vector of the FEM model which is arranged such that

$$\tilde{\phi}_k^{\text{FEM}}(\bar{\alpha}) = \begin{bmatrix} \tilde{\phi}_k^{\text{FEM,ext}}(\bar{\alpha})^\top & \tilde{\phi}_k^{\text{FEM},e}(\bar{\alpha})^\top \end{bmatrix}^\top \tag{33}$$

where $\tilde{\phi}_k^{\text{FEM,ext}}(\bar{\alpha})$ corresponds to the experimentally determined extended mode shape vector in (24) and $\tilde{\phi}_k^{\text{FEM},e}(\bar{\alpha})^\top$ contains the remaining unmeasured responses.

6.1.2. Algorithm

In this paper, an algorithm is considered that is based on the minimization of the difference in modal residuals

$$\hat{\bar{\alpha}} = \arg\min_{\bar{\alpha}} \sum_{k=1}^{n_m} \left(\left(\hat{\omega}_k - \tilde{\omega}_k^{\text{FEM}}(\bar{\alpha}) \right) W_{\omega,k} \right)^2$$
$$+ \left\| \left(\hat{\phi}_k^{\text{ext}} - \tilde{\phi}_k^{\text{FEM,ext}}(\bar{\alpha}) \right) W_{\phi,k} \right\|_2^2. \tag{34}$$

The considered cost function effectively minimizes the differences between the measured and predicted eigenfrequencies in (27) and mode shape vectors in (24). This cost function has been successfully used in structural dynamics applications including [35,37,39]. The modal damping parameters are not updated and the damping parameters identified in Section 5.1 are used. The optimization problem is solved iteratively using Gauss–Newton iterations, see Algorithm 1. For a more detailed explanation regarding the optimization, see, e.g., [39]. The resulting updated FEM model has a substantial model order $n_m \ll n_q$ which limits the suitability for applications. For this reason, model reduction is employed.

6.1.3. Spatio-temporal model

To obtain low-order spatio-temporal models, model reduction is employed, see, e.g., [36, Section 9.2.1]. In this paper, modal model reduction is considered by selecting modes that are relevant for control. The mass, stiffness, and damping matrices are then adjusted accordingly. The modal reduced model is defined as

$$\tilde{G}_m(s) = \sum_{k=1}^{n_m} \tilde{\phi}_k^{\text{FEM}}(\hat{\alpha}) \frac{1}{s^2 + d_{m,k}s + \tilde{\omega}_k^{\text{FEM}}(\hat{\alpha})^2} \tilde{\phi}_k^{\text{FEM,a}}(\hat{\alpha})^\top, \tag{35}$$

where $\tilde{\phi}_k^{\text{FEM,a}}(\hat{\alpha})$ denotes the part of the updated mode shape vector where the actuators are attached to the body. Due to the high spatial resolution of the mode shape vector $\tilde{\phi}_k^{\text{FEM}}(\hat{\alpha})$, the resulting modal model $\tilde{G}_m(s)$ provides detailed information about the spatial nature of the flexible dynamics. The resulting modal model can be converted through trivial transformations to the state-space form in (5) as shown in, e.g., [28].

7. Experimental case study

In this section, the effectiveness of the proposed approach is illustrated in an experimental case study. The case study includes a flexible beam setup, see Fig. 4. The case study encompasses all steps from frequency response function estimation to the formulation of the spatio-temporal model. The experimental setup is explained first. Second, the frequency response estimation procedure is discussed. Third, the identification of the modal model and the derivation of the extended modal model is discussed. Lastly, the spatio-temporal model is constructed. This section constitutes Contribution C2.

7.1. Experimental setup and aim

The experimental setup involves an overactuated beam setup with flexible dynamic behavior in mainly one dimension. The out-of-plane flexible dynamics is encountered in many applications, including, adaptive optics where the flexible dynamics is induced by the limited out-of-plane stiffness of the deformable mirror system and in wafer scanners where the limited out-of-plane stiffness of the motion stages leads to flexible dynamic behavior [8,9,30,63]. For this reason, the setup resembles a one-dimensional approximation of the multi-dimensional flexible dynamic behavior encountered in next-generation mechatronic systems.

The experimental overactuated beam setup is depicted in Fig. 4. The considered system is designed to exhibit out-of-plane flexible dynamic behavior. The system consists of a slim beam with dimensions $2 \times 20 \times 500$ mm. The system can be seen as to operate in 2 degrees of freedom, one translation, and one rotation. Four degrees of freedom are constrained by wire flexures. Due to the limited out-of-plane stiffness of the beam, the system contains a significant number of flexible modes. The beam system consists of three actuators and five sensors

$$G_f = \begin{bmatrix} f_1 & f_2 & f_3 \end{bmatrix} \mapsto \begin{bmatrix} u_1 & u_2 & u_3 & u_4 & u_5 \end{bmatrix} \tag{36}$$

where $u_i = u(\rho_{s,i})$, $i = 1, \ldots, 5$, where $\rho_{s,i}$ denotes the ith sensor location. The actuators f_i are Akribis AVM19-5 voice-coil actuators and the position is measured contactless with five Philtec D64-NQ fiberoptic
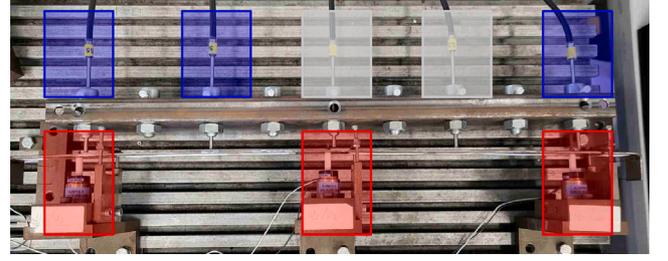
Fig. 4. Experimental overactuated beam setup. Three degrees of freedom are constrained by four vertical wire flexures, and one degree of freedom is constrained by a horizontal wire flexure (on the left). The setup is equipped with three voice coil actuators (🟥), five position sensors of which three are used for constructing the spatio-temporal model (🟦) and two sensors are used for validation purposes (⬛).

sensors, with a resolution of 1 μm. A Beckhoff EtherCAT module is used for data acquisition and the system operates with a sampling frequency of 2048 Hz.

The measured positions are relative with respect to a steel bracket. These measurements are approximately be absolute due to the high stiffness of the bracket, the rigid and heavy test bench, and the bracket not being in the force loop. Similarly, each actuator exerts a force relative to an independent heavy steal bracket which is mounted to a heavy and rigid table.

The aim is to estimate a spatio-temporal model of the beam system in Fig. 4

$$G_o(\rho) : \begin{bmatrix} f_1 & f_2 & f_3 \end{bmatrix} \mapsto u(\rho), \quad \rho \in \mathcal{S}, \tag{37}$$

where $u(\rho)$, $\rho \in \mathcal{S}$, denotes the deflection function on the domain $\mathcal{S}$. To illustrate the effectiveness of the proposed approach, an overactuated setting with limited sensing capabilities is created, i.e.,

$$G_s : \begin{bmatrix} f_1 & f_2 & f_3 \end{bmatrix} \mapsto \begin{bmatrix} u_1 & u_2 & u_5 \end{bmatrix}. \tag{38}$$

Thus, only three position sensors are used to estimate the spatio-temporal model. It is emphasized that the remaining two sensors are used for validation purposes only.

7.2. Experimental results: Step 1: Frequency response function estimation

To identify the spatio-temporal model, first, the frequency response function is estimated. Since the system is stable and has a certain limited stroke, open-loop experiments are conducted. A full-MIMO random phase multisine input signal with a flat amplitude spectrum is injected into all inputs up to the Nyquist frequency. The excitation signal contains 12 period with independent 30 realizations with a total measurement time of approximately one hour. The results are processed with spectral analysis in Matlab. The identified element-wise Bode magnitude plot of the frequency response function estimate is depicted in Fig. 5.

7.3. Step 2.1: Modal model identification

This subsection aims to identify a parametric modal model of the spatially sampled system G_s. Modal models are estimated of the form in (13). For control, low-order models are desired that are sufficiently accurate in the control-relevant frequency range. For this reason, the first $n_m = 9$ modes are considered which cover most of the dynamics that are relevant for control.

To identify the modal model of the form in (13), the optimization algorithm outlined in Section 5.1 is used. An inverse Schur weighting filter W_s is designed in (18) to emphasize the relative difference between the frequency response function of the modal model, see [28, Section IV.B]. The input weighting filter W_f is a first-order filter with
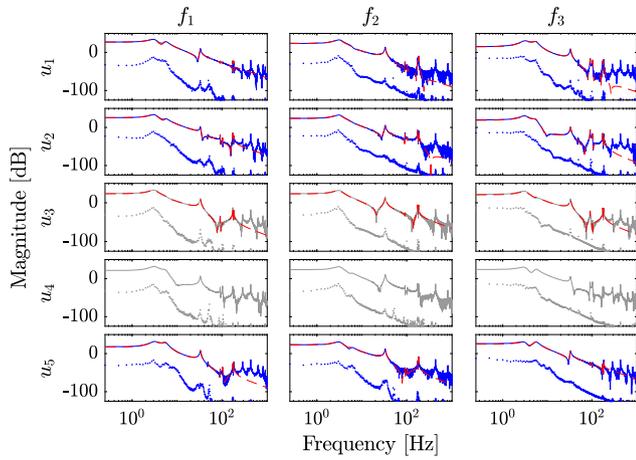
Fig. 5. Element-wise Bode magnitude plot of the frequency response function estimate of the full system G_f (———) and the subset G_s (———) and their corresponding variances (same colors, dotted), and the identified parametric extended plant $\hat{G}_{ext}$ (– – –). It is emphasized that the extended plant is estimated using the frequency response function estimate of the subsystem G_s only whereas the full system G_f is only shown for validation purposes.

Fig. 6. Rendering of the finite element mesh used to construct the spatio-temporal identification of the flexible beam. The mesh incorporates the folded ends of the beam and includes five wire flexures. The FEM model employs 4000 elements to capture the dynamics of the beam setup.

a cutoff of 200 Hz to emphasize low frequencies. The output weighting filter W_u is set to identity.

The resulting element-wise Bode magnitude plot of the modal model $\hat{G}_s$ is depicted in Fig. 5. The plot reveals that the modal model accurately fits the frequency response function estimate. However, the analysis of the modal model in its current form is limited to a temporal analysis of three sensors, which limits the spatial resolution. For this reason, the construction of the extended modal model is essential.

7.4. Step 2.2: Extended modal model

An important step in the estimation of the spatio-temporal model is to construct the extended modal model as outlined in Section 5.2. Since the first sensor is collocated with the first actuator, the conditions underlying Theorem 2 are satisfied. Consequently, the identified modal participation matrix is uniquely decomposed into mass-normalized mode shape vectors. Another important step in the formulation of the extended modal model is to combine the mode shape vectors sampled at the sensor and actuator positions in (24). The extended modal model is constructed in (27) and (28). These mode shape vectors are visualized in Fig. 8. The resulting element-wise Bode magnitude plot is depicted in Fig. 5. The spatial resolution of the extended modal model is increased without having additional sensors. This is an important step in the identification of the spatio-temporal model.

In Fig. 5, an Element-wise Bode magnitude plot is depicted of the frequency response function estimate, the modal model, and the extended modal model. The modal and extended modal models accurately match the frequency response function estimate. This confirms the capability of the modal model identification algorithm in Section 5.1 to accurately identify modal models and the validity formulation of the extended modal model in Section 5.2. A discrepancy in the response at sensors 3 and 5 between the extended modal model and the frequency response estimate appears in the vicinity of the modes at 572 Hz and 649 Hz. The FEM model indicates that these frequencies match with an in-plane mode. As a consequence of a tilted sensor and a significant bend in the beam, the in-plane mode appears in the frequency response function estimate. Overall, the extended modal model accurately matches the frequency response estimate and enables the prediction of the dynamic behavior at the third sensor without using the frequency response function estimate. Hence, the extended modal
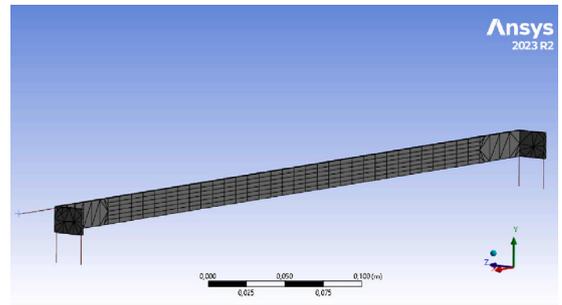
model enables an enhancement of the spatial resolution without additional sensors. It is emphasized that the frequency response function estimates at sensors 3 and 4 are only used for validation purposes.

7.5. Experimental results: Step 4: Spatio-temporal model

Similar to many overactuated mechatronic systems in practice, a detailed FEM model is available of the flexible beam setup. The FEM model is made in Ansys, see Fig. 6. A three-dimensional model with 4000 elements of the flexible beam setup is considered including the folded end tips and the wire flexures. Although the model covers a substantial amount of detail of the flexible beam, there are a few non-modeled artifacts, including, several buckled wire flexures, the slight bend in the beam, and the actuators.

The spatio-temporal model is constructed by updating a prior FEM model based on the extended modal model. The geometry of the model is depicted in Fig. 6. The model is parameterized by five update parameters

$$\bar{\alpha} = \begin{bmatrix} E, \rho, \nu, k_1, k_2, \end{bmatrix} \tag{39}$$

where, E, ρ, and ν denote the Young modulus, mass density, and Poisson ratio of the flexible beam, respectively, and, k_1 and k_2 the stiffness of the vertical and horizontal wire flexures, respectively. The update parameters are optimized by the procedure outlined in Section 6.1. The element-wise Bode magnitude plot of the initial and updated spatio-temporal model at the five sensor locations is depicted in Fig. 7.

In Fig. 7, the estimate of the spatio-temporal model is depicted in the element-wise Bode magnitude plot. The initial non-updated model significantly overestimates the eigenfrequencies. This is likely caused by imperfections in the beam setup, e.g., buckled wire flexures and a bent flexible beam. In contrast, the updated model accurately matches the frequency response function estimate. In particular, the updated model accurately captures the low-order modes including rigid-body modes and the first flexible mode. The modes at 572 Hz and 649 Hz in the frequency response function estimate are attributed to an in-plane mode according to the FEM model. Due to sensor tilt or misalignment with the beam, this behavior is observed in the frequency response estimate of the out-of-plane sensors. Therefore, these modes are not visible in the out-of-plane directions of the model. It is emphasized that only the frequency response function estimate of three sensors are used for identifying the spatio-temporal model. This confirms the effectiveness of the proposed approach to identify the spatio-temporal behavior of overactuated mechatronic systems with a limited number of sensors.

Fig. 8 depicts the mode shape vectors for six modes based on the extended modal model, the initial non-updated FEM model, and the updated spatio-temporal model. The initial non-updated model deviates
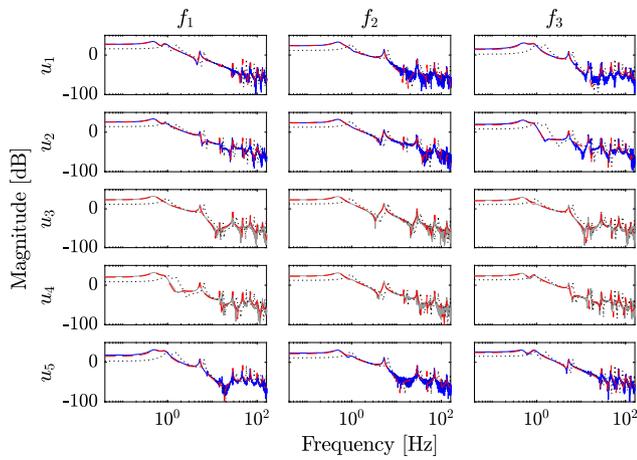
Fig. 7. Element-wise Bode magnitude plot of the frequency response function estimate of the full system G_{f} (——) and the subset G_{s} (——) and the initial FEM model (••••) and the spatio-temporal model $\tilde{G}_m$ (——). It is emphasized that the spatio-temporal model is essentially obtained using the non-parametric estimate of the subsystem only and the full system G_{f} is only visualized for validation purposes.
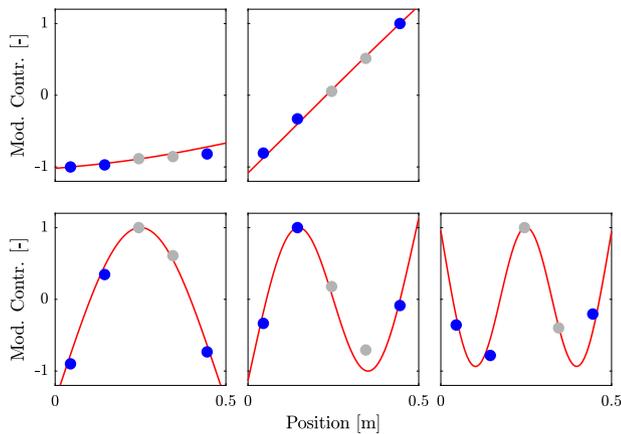
Fig. 8. Visualization of the mode shape vectors corresponding to the rigid-body modes (top) and the flexible modes (bottom) mode of the flexible beam. Visualized are the mode shape vector based on a modal model of the full system (⬤), and subsystem (⬤). The spatio-temporal model (——) demonstrates accurate estimation of the flexible dynamic behavior. The position coordinate reflects the horizontal position on the flexible beam.

significantly from the extended modal model. In contrast, the updated model accurately matches the extended mode shape vectors. Overall, the experimental case study illustrates that the proposed approach enables accurate identification of the spatio-temporal system behavior of overactuated mechatronic systems with a limited number of spatially distributed sensors.

In Fig. 9, the measured step response, the step response simulated with the non-updated FEM model, and the simulated step response based on the spatio-temporal model at the location of the fourth sensor are depicted. The system is perturbed with a step response in the direction of the first flexible mode. The response of the spatio-temporal model matches the measured response relatively well. The response confirms that the rigid-body modes and the first flexible mode are accurately modeled as indicated in Fig. 7. However, the steady-state response somewhat deviates from the measured response. This can be caused by the compliance effect of high-order modes that is not included in the spatio-temporal model.
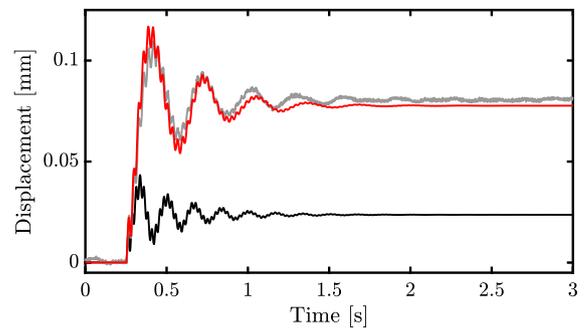
Fig. 9. Step response at sensor 4. The plot depicts the validation data (——), non-updated FEM model (——), and spatio-temporal model (——). It is emphasized that the validation data is solely used for validation purposes and is not used to identify the spatio-temporal model.

8. Discussion

The proposed spatio-temporal modeling approach encompasses all steps from frequency response function estimation, modal model identification, and extended modal model construction to spatio-temporal modeling using prior FEM models. The experimental results confirm the ability of the proposed approach to accurately model the spatio-temporal behavior.

In comparison to previous studies, the approach proposed in this paper offers several advantages. First, the results presented in this paper extend to the previous results in [43,63] by providing an approach for modeling the spatio-temporal system behavior, an extended derivation of the modal modeling framework, and the identification of the (extended) modal models is automated through an optimization algorithm. Secondly, a frequency domain-based approach is pursued which enables enhanced data efficiency, interpretability for control, and model validation in view of control compared to time domain methods [64–66]. Thirdly, in [28,56], a two-stage optimization procedure is required to obtain an appropriate initial estimate for the second Gauss–Newton iteration stage. This paper identifies modal models with a single stage Gauss–Newton algorithm by using an initial estimate based on prior system knowledge which reduces the computational effort. Similar to the two-stage algorithms, the algorithm considered in this paper does not necessarily converge to the global optimum. However, the results presented in this paper illustrate that it works well in practice. The initial estimate procedure may lead to insufficiently inaccurate results in the case of significant coupling between the modes and leads to a slight increase in user intervention. However, the procedure works well in practice as shown in, e.g., [57]. Fourthly, the estimation quality of traditional experimental approaches to identify a spatio-temporal model is limited by the finite number of sensors that capture the complex spatial nature of the flexible dynamics [28,37,67]. In contrast, the approach in this paper exploits the symmetric nature of the mode shape vectors at actuator and sensor level. By combining these mode shape vectors, the spatial resolution of the obtained extended modal model is enhanced which leads to an enhanced spatio-temporal estimation quality of the spatio-temporal model [43]. Finally, in contrast to the field of structural analysis (e.g., [56,68]), the focus in this paper lies on obtaining spatio-temporal models that are suitable for control purposes. This is emphasized by the possibility of extending the proposed approach to incorporate control-relevant identification criteria [14]. Furthermore, a unified approach is proposed from frequency response measurements to the identification of modal models and spatio-temporal models. Similar to the optimization algorithm of the parametric modal model, the model updating algorithm does not need to converge to the global optimum. The results reported in this paper and the literature (e.g.,[37]) indicate that these algorithms seem to work well in practice. However, experience with the considered

setup indicated that the quality of the updated model depends on the considered parameterized finite-element model. Hence, the considered FEM model should be contain a sufficient amount of detail of the considered setup. The required level of detail depends on the considered application and must be balanced with the increased computational complexity. The number and selection of the update parameters must be considered based on the relevancy for the update problem, also sensitivity methods can be used to automate this process [36]. For complex geometries and increased automation, mode tracing and mode matching techniques can also be considered see, e.g., [36,47].

Alternatively, the development of port-Hamiltonian system analysis has spurred the development of port-Hamiltonian control strategies for mechanical systems [16,17]. In this paper, FEM models and a frequency domain-based approach are considered as these are usually the starting point in the mechatronic industry. In particular, software packages for FEM analysis are available on a wide scale and are widely used in the mechatronic industry. These models can be combined with experimental data, i.e., model updating, to compensate for, e.g., overestimation of the stiffness resulting in overestimated eigenfrequencies and variations across systems due to manufacturing tolerances. The resulting spatio-temporal models are accurate and relatively accessible for mechatronic engineers due to the wide adoption of FEM software packages. Furthermore, a frequency domain-based approach is considered as these frequency domain-based approaches are widely adopted in mechatronic system design. These frequency-domain approaches are well established and naturally align with control-relevant system identification techniques, as demonstrated in, e.g., [14]. However, alternatively, partial differential equations-based and port-Hamiltonian-based approaches can also be considered to describe the flexible dynamic behavior.

The proposed framework is tailored to systems of the form in (11). In particular, mechatronic systems that consist of a single moving body. However, it is envisioned that the proposed approach is also applicable to systems with more than one flexible body. An example of such a system is a deformable mirror system with a flexible actuator support frame, as shown in [43]. Ongoing research focuses on confirming the performance and applicability of the proposed approach for these systems. The ability of the proposed approach to model unmeasured sensor locations is confirmed in Section 7.5 and in particular in Figs. 7 and 9. However, the proposed framework is not yet used in a control setting. For this reason, ongoing research focuses on using the proposed spatio-temporal modeling method in inferential control approaches. The spatio-temporal modeling approach is expected to enhance the performance of inferential control algorithms in next-generation motion technologies using the methodologies in, e.g., [3,15,69–71].

9. Conclusions

This paper presents an approach to identify spatio-temporal models for control of overactuated mechatronic systems with a limited number of sensors. An important step is to employ prior system knowledge through the modal modeling framework and prior FEM models.

A frequency domain-based approach is pursued for efficient and interpretable data processing in Section 4. In Section 5, modal models are identified that describe the spatially-sampled input–output behavior. The identification algorithm is based on a single-step Gauss–Newton approach with an initial guess based on the frequency response function estimate. The spatial resolution of the modal models is enhanced by exploiting the symmetry of modal models in Section 5.2. Spatio-temporal models are identified by updating prior FEM models through the identified extended modal models in Section 6. The integration of prior knowledge from mechanical models and FEM models leads to accurate spatio-temporal models. The experimental results confirm that the proposed method is able to accurately capture the spatio-temporal system behavior and accurately estimate the dynamic behavior at unmeasured sensor locations

CRediT authorship contribution statement

Paul Tacx: Writing – review & editing, Writing – original draft, Visualization, Software, Methodology, Formal analysis, Data curation, Conceptualization. **Matthijs van de Vosse:** Writing – original draft, Software, Methodology, Data curation, Conceptualization. **Robbert Voorhoeve:** Writing – review & editing, Writing – original draft, Methodology, Formal analysis, Conceptualization. **Gert Witvoet:** Writing – review & editing, Writing – original draft, Methodology, Conceptualization. **Marcel Heertjes:** Writing – review & editing, Writing – original draft, Methodology, Conceptualization. **Tom Oomen:** Writing – review & editing, Writing – original draft, Resources, Methodology, Formal analysis, Conceptualization.

Declaration of competing interest

The authors declare that they have no known competing financial interests or personal relationships that could have appeared to influence the work reported in this paper.

Appendix. Proof of Theorem 2

Proof. Let R_k be a rank-one modal participation matrix and let $\rho_{s,i} = \rho_{a,j}$ for a certain collocated index pair $i, j \in \mathbb{N}$ be the collocated positions of the sensor-actuator pair. As such, the mass-normalized mode shape vectors are related through

$$[v_k]_i = [w_k]_j. \tag{A.1}$$

Here, $[.]_i$ denotes the ith element of a vector. By virtue of Theorem 1, the rank-one modal participation matrix can be decomposed into a dyadic product of mode shape vectors $\bar{v}_k$, and $\bar{w}_k$ which are unique up to a scaling parameter β

$$R_k = \beta \bar{v}_k \frac{1}{\beta} \bar{w}_k^\top. \tag{A.2}$$

These mode shape vectors are mass-normalized by finding the scaling parameter β^* such that

$$v_k = \beta^* \bar{v}_k \quad w_k = \frac{1}{\beta^*} \bar{w}_k \tag{A.3}$$

Substitution of (A.1) in (A.3) and subsequent reformulation leads to the scaling parameter

$$\beta^* = \sqrt{\frac{[\bar{w}_k]_j}{[\bar{v}_k]_i}} \tag{A.4}$$

which mass-normalizes any arbitrarily scaled mode shape vectors $\bar{v}_k$, and $\bar{w}_k$ and completes the proof of Theorem 2. $\square$

Data availability

The authors are unable or have chosen not to specify which data has been used.

References

[1] Balas MJ. Active control of flexible systems. J Optim Theory Appl 1978;25(3):415–36.

[2] Schneiders M, Van De Molengraft M, Steinbuch M. Benefits of overactuation in motion systems. In: Proceedings of the 2004 American control conference. vol. 1, IEEE; 2004, p. 505–10.

[3] Moheimani SOR, Fleming AJ, Halim D. Spatial control of vibration: theory and experiments. World Sci 2003;10.

[4] Kuiper S, Doelman N, Human J, Saathof R, Klop W, Maniscalco M. Advances of tno's electromagnetic deformable mirror development. In: Advances in optical and mechanical technologies for telescopes and instrumentation. vol. 10706, SPIE; 2018, p. 345–52.

[5] Hamelinck R, Ellenbroek R, Rosielle N, Steinbuch M, Verhaegen M, Doelman N. Validation of a new adaptive deformable mirror concept. In: Adaptive optics systems. vol. 7015, SPIE; 2008, p. 163–74.

[6] Beckers J. Adaptive optics for astronomy: principles, performance, and applications. Annu Rev Astron Astrophys 1993;31(1):13–62.

[7] Booth M. Adaptive optics in microscopy. Phil Trans R Soc A 2007;365(1861):2829–43.

[8] van deWal M, van Baars G, Sperling F, Bosgra O. Multivariable $\mathcal{H}_\infty \mu$ feedback control design for high-precision wafer stage motion. Control Eng Practice 2002;10(7):739–55.

[9] Tacx P, Oomen T. A one-step approach for centralized overactuated motion control of a prototype reticle stage. In: IFAC modeling, estimation, and control conference. MECC, 2022, p. 308–13.

[10] Schmidt RM, Schitter G, Rankers A. The design of high performance mechatronics-: high-tech functionality by multidisciplinary system integration. Ios Press; 2020.

[11] Chiuso A, Muradore R, Marchetti E. Dynamic calibration of adaptive optics systems: A system identification approach. IEEE Trans Control Syst Technol 2009;18(3):705–13.

[12] Coronel M, Soto N, Carvajal R, Escárate P, Agüero JC. Identification and model predictive control of an experimental adaptive optics setup utilizing Kautz basis functions. In: Adaptive optics systems VII. vol. 11448, SPIE; 2020, p. 497–508.

[13] Heertjes MF, Butler H, Dirkx N, Van Der Meulen S, Ahlawat R, O'Brien others. Control of wafer scanners: Methods and developments. In: American control conference. ACC, IEEE; 2020, p. 3686–703.

[14] Oomen T, van Herpen R, Quist S, Van De Wal M, Bosgra O, Steinbuch M. Connecting system identification and robust control for next-generation motion control of a wafer stage. IEEE Trans Control Syst Technol 2013;22(1):102–18.

[15] Oomen T, Grassens E, Hendriks F. Inferential motion control: Identification and robust control framework for positioning an unmeasurable point of interest. IEEE Trans Control Syst Technol 2014;23(4):1602–10.

[16] Ponce C, Ramirez H, Le Gorrec Y. Finite dimensional shape control design of linear port-hamiltonian systems with in-domain pointwise inputs. IFAC-PapersOnLine 2023;56(2):6777–82.

[17] Liu N, Wu Y, Le Gorrec Y, Lef'evre L, Ramirez H. Reduced order in domain control of distributed parameter port-hamiltonian systems via energy shaping. Automatica 2024;161:111500.

[18] da Silva MM, Desmet W, Van Brussel H. Design of mechatronic systems with configuration-dependent dynamics: simulation and optimization. IEEE/ASME Trans Mechatronics 2008;13(6):638–46.

[19] Ronde M, van de Molengraft R, Steinbuch M. Model-based feedforward for inferential motion systems, with application to a prototype lightweight motion system. In: 2012 American Control Conference (ACC). IEEE; 2012, p. 5324–9.

[20] Papageorgiou G, Glover K, D'Mello G, Patel Y. Taking robust lpv control into flight on the vaac harrier. In: Proceedings of the 39th IEEE conference on decision and control (Cat. No. 00CH37187). vol. 5, IEEE; 2000, p. 4558–64.

[21] Wassink MG, van de Wal M, Scherer C, Bosgra O. Lpv control for a wafer stage: beyond the theoretical solution. Control Eng Pract 2005;13(2):231–45.

[22] Scherer CW. Lpv control and full block multipliers. Automatica 2001;37(3):361–75.

[23] Van Wingerden J-W, Verhaegen M. Subspace identification of bilinear and LPV systems for open-and closed-loop data. Automatica 2009;45(2):372–81.

[24] Bamieh B, Giarre L. Identification of linear parameter varying models. Int J Robust Nonlinear Control 2002;12(9):841–53.

[25] Voss H, Bünner M, Abel M. Identification of continuous, spatiotemporal systems. Phys Rev E 1998;57(3):2820.

[26] van Kampen RJR, van Berkel M, Zwart H. Estimating spacedependent coefficients for 1d transport using gaussian processes as state estimator in the frequency domain. IEEE Control Syst Lett 2022;7:247–52.

[27] Morris K, Levine W. Control of systems governed by partial differential equations. In: The control theory handbook. 2010.

[28] Voorhoeve R, de Rozario R, Aangenent W, Oomen T. Identifying position-dependent mechanical systems: A modal approach applied to a flexible wafer stage. IEEE Trans Control Syst Technol 2020;29(1):194–206.

[29] Ruppel T, Osten W, Sawodny O. Model-based feedforward control of large deformable mirrors. Eur J Control 2011;17(3):261–72.

[30] Ruppel T, Dong S, Rooms F, Osten W, Sawodny O. Feedforward control of deformable membrane mirrors for adaptive optics. IEEE Trans Control Syst Technol 2012;21(3):579–89.

[31] Ronde MJC, Schneiders MGE, Kikken EJGJ, Van De Molengraft MJG, Steinbuch M. Model-based spatial feedforward for overactuated motion systems. Mechatronics 2014;24(4):307–17.

[32] Gasmi R, Le Bihan D, Dournaux J-L, Sinquin J, Jagourel P. Active control of a large deformable mirror for future E-ELT. In: Adaptive optics systems. vol. 7736, SPIE; 2010, p. 505–15.

[33] Oya S, Bouvier A, Guyon O, Watanabe M, Hayano Y, Takami H, et al. Performance of the deformable mirror for subaru LGSAO. In: Advances in adaptive optics II. vol. 6272, SPIE; 2006, p. 1523–30.

[34] Haber A, Verhaegen M. Modeling and state-space identification of deformable mirrors. Opt Express 2020;28(4):4726–40.

[35] Mottershead JE, Friswell MI. Model updating in structural dynamics: a survey. J Sound Vib 1993;167(2):347–75.

[36] Friswell M, Mottershead JE. Finite element model updating in structural dynamics. vol. 38, Springer Science & Business Media; 1995.

[37] Dorosti M, Fey R, Heertjes M, van de Wal M, Nijmeijer H. Finite element model reduction and model updating of structures for control. IFAC Proc Vol 2014;47(3):4517–22.

[38] Steenackers G, Guillaume P. Finite element model updating taking into account the uncertainty on the modal parameters estimates. J Sound Vib 2006;296(4–5):919–34.

[39] Mottershead JE, Link M, Friswell MI. The sensitivity method in finite element model updating: A tutorial. Mech Syst Signal Process 2011;25(7):2275–96.

[40] Li W-M, Hong J-Z. Research on the iterative method for model updating based on the frequency response function. Acta Mech Sin 2012;28(2):450–7.

[41] Pradhan S, Modak S. Normal response function method for mass and stiffness matrix updating using complex frfs. Mech Syst Signal Process 2012;32:232–50.

[42] Rahmatalla S, Eun H-C, Lee E-T. Damage detection from the variation of parameter matrices estimated by incomplete frf data. Smart Struct Syst 2012;9(1):55–70.

[43] Tacx P, Teurlings M, Habraken R, Witvoet G, Heertjes MF, Oomen T. Spatio-temporal analysis of overactuated motion systems: A mechanical modeling approach. In: IFAC world triennial world congress. 2023, p. 8784–9.

[44] Maxwell JC. On the calculation of the equilibrium and stiffness of frames. Philos Mag J Sci 1864;27(182):598–604.

[45] Betti E. Teoria della elasticita. In: Il nuovo cimento (1869-1876). vol. 7, (1):1872, p. 291–378.

[46] Ghali A, Neville AM. Structural analysis: a unified classical and matrix approach. Crc Press; 1972.

[47] Gawronski WK. Advanced structural dynamics and active control of structures. Springer; 2004.

[48] Voorhoeve R, van der Maas A, Oomen T. Non-parametric identification of multivariable systems: A local rational modeling approach with application to a vibration isolation benchmark. Mech Syst Signal Process 2018;105:129–52.

[49] Pintelon R, Schoukens J, Vandersteen G, Barb'e K. Estimation of nonparametric noise and frf models for multivariable systems—part i: Theory. Mech Syst Signal Process 2010;24(3):573–95.

[50] Garnier H, Wang L, Young PC. Direct identification of continuoustime models from sampled data: Issues, basic solutions and relevance. In: Identification of continuous-time models from sampled data. Springer; 2008, p. 1–29.

[51] Pintelon R, Schoukens J. System identification: a frequency domain approach. John Wiley & Sons; 2012.

[52] Kontaras N, Heertjes MF, Zwart H. Continuous compliance compensation of position-dependent flexible structures. IFAC-PapersOnLine 2016;49(13):76–81.

[53] Craig Jr. RR, Kurdila AJ. Fundamentals of structural dynamics. John Wiley & Sons; 2006.

[54] Levy EC. Complex-curve fitting. IRE Trans Autom Control 1959;4(1):37–43.

[55] Oomen TAE. System identification for robust and inferential control: with applications to ilc and precision motion systems. 2010.

[56] Reynders E. System identification methods for (operational) modal analysis: review and comparison. Arch Comput Methods Eng 2012;19(1):51–124.

[57] Witvoet G, den Breeje R, Nijenhuis J, Hazelebach R, Doelman N. Dynamic analysis and control of mirror segment actuators for the european extremely large telescope. J Astron Telesc Instrum Syst 2015;1(1):019003.

[58] Brincker R, Zhang L, Andersen P. Modal identification from ambient responses using frequency domain decomposition. In: IMAC 18: proceedings of the international modal analysis conference (IMAC), San Antonio, Texas, USA, February (2000) 7–10. 2000, p. 625–30.

[59] Axler S. Linear algebra done right. Springer Science & Business Media; 1997.

[60] Shores TS, et al. Applied linear algebra and matrix analysis. vol. 2541, Springer; 2007.

[61] Richardson MH, Jamestown C. Modal mass, stiffness and damping. Jamestown, CA: Vibrant Technology, Inc; 2000, p. 1–5.

[62] Ewins DJ. Modal testing: theory, practice and application. John Wiley & Sons; 2009.

[63] Tacx P, Habraken R, GWitvoet, Heertjes MF, Oomen T. Identification of an overactuated deformable mirror system with unmeasured outputs. IFAC Mechatron 2024;99:103158.

[64] Pintelon R, Guillaume P, Rolain Y, Schoukens J, Van Hamme H. Parametric identification of transfer functions in the frequency domain-a survey. IEEE Trans Autom Control 1994;39(11):2245–60.

[65] Poulimenos AG, Fassois SD. Parametric time-domain methods for non-stationary random vibration modelling and analysis—a critical survey and comparison. Mech Syst Signal Process 2006;20(4):763–816.

[66] Verboven P. Frequency-domain system identification for modal analysis [Ph.D. thesis], Brussels: Vrije Universiteit Brussel; 2002.

[67] Kilpatrick J, Apostol A, Khizhnya A, Markov V, Beresnev L. Realtime characterization of the spatio-temporal dynamics of deformable mirrors. In: Laser communication and propagation through the atmosphere and oceans v. vol. 9979, SPIE; 2016. p. 34–45.

[68] Zhang L, Brincker R. An overview of operational modal analysis: major development and issues. In: Proceedings of the 1st international operational modal analysis conference, April 26–27, 2005, Copenhagen, Denmark. Aalborg Universitet; 2005. p. 179–90.

[69] Voorhoeve R, Dirkx N, Melief T, Aangenent W, Oomen T. Estimating structural deformations for inferential control: a disturbance observer approach. In: IFAC symposium on mechatronic systems. vol. 49, IFAC; 2016. p. 642–8.

[70] Parrish J, Brosilow C. Inferential control applications. Automatica 1985;21(5):527–38.

[71] Doyle III FJ. Nonlinear inferential control for process applications. J Process Control 1998;8(5–6):339–53.

Paul Tacx received the M.Sc. (cum laude) and Ph.D. degrees in Mechanical Engineering from the Eindhoven University of Technology, Eindhoven, The Netherlands, in 2019 and 2024, respectively. He is currently a post-doctoral researcher with the Department of Mechanical Engineering at the Eindhoven University of Technology. His research interests include identification and control of overactuated mechatronic systems.

Matthijs van de Vosse received the M.Sc degree in Mechanical Engineering from the Eindhoven University of Technology, Eindhoven, the Netherlands, in 2024. He is currently a design engineer at Damen Shipyards Group.

Robbert Voorhoeve received the M.Sc. degree in Mechanical Engineering (cum laude) and Applied Physics in 2013 and his Ph.D. degree in Mechanical Engineering in 2018 from the Eindhoven University of Technology, Eindhoven, The Netherlands. He is currently a dynamics and control specialist engineer at the Netherlands Organisation for Applied Scientific Research (TNO), Delft, The Netherlands. His research interests include system identification, identification for advanced motion control, and control of complex mechatronic systems.

Gert Witvoet received the M.Sc. (cum laude) and Ph.D. degrees from the Eindhoven University of Technology, Eindhoven, The Netherlands, in 2007 and 2011, respectively. He is currently a Senior Dynamics and Control Specialist at the Netherlands Organisation for Applied Scientific Research (TNO), Delft, The Netherlands, and a part-time Assistant Professor with the Mechanical Engineering Department, Eindhoven University of Technology. His research interest includes the application of advanced motion control techniques on high-tech instruments and applications in the semiconductor, astronomy, and space markets. Dr. Witvoet is a recipient of the Unilever Research Prize and several best master teacher awards.

Marcel Heertjes received the M.Sc. and Ph.D. degrees from the Eindhoven University of Technology, Eindhoven, The Netherlands, in 1995 and 1999, respectively. After being with the Philips Center for Industrial Technology from 20002005, he joined ASML in 2006. He was a recipient of the IEEE Control Systems Technology Award 2015 for variable gain control and its applications to wafer scanners. In 2019, he was appointed full Professor on Industrial Nonlinear Control for High-Precision Systems at Eindhoven University of Technology. He acts as an Associate Editor for IFAC Mechatronics since 2016. Regarding his work on hybrid integrator-gain systems, he was a recipient of the IFAC Automatica paper prize award 2023.

Tom Oomen is full professor with the Department of Mechanical Engineering at the Eindhoven University of Technology. He is also a part-time full professor with the Delft University of Technology. He received the M.Sc. degree (cumlaude) and Ph.D. degree from the Eindhoven University of Technology, Eindhoven, The Netherlands. He held visiting positions at KTH, Stockholm, Sweden, and at The University of Newcastle, Australia. He is a recipient of the 7th Grand Nagamori Award, the Corus Young Talent Graduation Award, the IFAC 2019 TC 4.2 Mechatronics Young Research Award, the 2015 IEEE Transactions on Control Systems Technology Outstanding Paper Award, the 2017 IFAC Mechatronics Best Paper Award, the 2019 IEEJ Journal of Industry Applications Best Paper Award, and recipient of a Veni and Vidi personal grant. He is currently a Senior Editor of IEEE Control Systems Letters (L-CSS) and Associate Editor of IFAC Mechatronics, and he has served on the editorial boards of the IEEE Control Systems Letters (L-CSS) and IEEE Transactions on Control Systems Technology. He has also been vice-chair for IFAC TC 4.2 and a member of the Eindhoven Young Academy of Engineering. His research interests are in the field of data-driven modeling, learning, and control, with applications in precision mechatronics.